

Focusing Mutations into the *P. fluorescens* Esterase Binding Site Increases Enantioselectivity More Effectively than Distant Mutations

Seongsoon Park,^{1,2} Krista L. Morley,¹
Geoff P. Horsman,^{1,3} Mats Holmquist,^{2,4}
Karl Hult,² and Romas J. Kazlauskas^{1,5,*}

¹Department of Chemistry
McGill University
801 Sherbrooke Street, West
Montréal, Québec H3A 2K6
Canada

²Department of Biotechnology
Royal Institute of Technology (KTH)
AlbaNova University Center
Roslagstullsbacken 21
SE-106 91 Stockholm
Sweden

Summary

Rational design of enzymes with improved properties, such as enantioselectivity, usually focuses mutations within the substrate binding site. On the other hand, directed evolution of enzymes usually targets the entire protein and discovers beneficial mutations far from the substrate binding site. In this paper, we propose an explanation for this discrepancy and show that a combined approach—random mutagenesis within the substrate binding site—is better. To increase the enantioselectivity (*E*) of a *Pseudomonas fluorescens* esterase (PFE) toward methyl 3-bromo-2-methylpropionate, we focused mutagenesis into the substrate binding site at Trp28, Val121, Phe198, and Val225. Five of the catalytically active mutants (13%) showed better enantioselectivity than wild-type PFE. The increases in enantioselectivity were higher (up to 5-fold, reaching *E* = 61) than with mutants identified by random mutagenesis of the entire enzyme.

Introduction

Changing an enzyme's catalytic properties, such as enantioselectivity, is an important practical goal. Enzymes with high enantioselectivity toward unnatural substrates help chemists make key pharmaceutical intermediates. In addition, these changes can also reveal mechanistic information on the molecular basis for catalytic power and stereoselectivity of enzymes.

In the last decade, several groups increased the enantioselectivity of an enzyme by directed evolution—repeated random mutagenesis and screening of mutants for improved properties [1–16]. For example, Rietz's and Jaeger's groups increased the enantioselectivity of *Pseudomonas aeruginosa* lipase (PAL) from

E = 1.1 to *E* = 26 toward an unnatural substrate by using four cycles of random mutagenesis and screening [11]. Similarly, we moderately increased the enantioselectivity of an esterase from *Pseudomonas fluorescens* (PFE) from *E* = 12 to *E* = 19 by random mutagenesis and screening [15].

Surprisingly, the enantioselectivity-increasing mutations discovered in these experiments lie far from the enzyme active site (Figure 1A). The observed enantioselectivity changes are given as activation energy differences ($\Delta\Delta\Delta G^\ddagger$) to simplify comparison. (The three deltas stem from the following. The activation free energy change for a chemical reaction is given by ΔG^\ddagger . Enantioselectivity compares the reactivity of the enantiomers and is given by $\Delta\Delta G^\ddagger = -RT\ln E$. Enantioselectivity changes caused by mutations compare the enantioselectivity before and after mutation and are given by $\Delta\Delta\Delta G^\ddagger = -RT\ln[E_{\text{mutant}}/E_{\text{wild-type}}]$). Typically, the C α of the mutated amino acid lies 12–14 Å from the stereocenter of the substrate. The closest contact distance may be shorter, depending on the side chain orientation. These distant changes increase enantioselectivity by propagating structural changes to the substrate binding site. In many cases, directed evolution uses multiple mutations to alter or even invert enantioselectivity [17], but we excluded these examples because we cannot assign the enantioselectivity change to one amino acid. In contrast, rational designs to increase enantioselectivity always target the substrate binding site, usually within 10 Å of the substrate's stereocenter [18–22]. For example, the Gly60Ala mutation in a phosphotriesterase, which increased the enantioselectivity from 21 to 11,000 for hydrolysis of *p*-nitrophenyl ethyl phenyl phosphate, was at most 7.6 Å from the phosphorus stereocenter [22]. Why does directed evolution usually discover distant and not close mutations?

Fully random mutagenesis would create all possible combinations of the 19 natural amino acids at each position in a protein. However, this is an impossibly large number of possibilities—for a 300 amino acid protein, it is larger than the number of atoms in the universe—so experimental design limits the randomness in all random mutagenesis experiments. We refer to all mutagenesis experiments that contain some randomness as random mutagenesis. We distinguish between methods that act on the entire protein from those that act in a more limited region. For example, error-prone PCR generates amino acid substitutions by targeting the entire protein. Likewise, DNA shuffling targets the entire protein by exchanging fragments of related proteins. On the other hand, saturation mutagenesis acts in a limited region because it replaces amino acids in selected sites with each of the 19 natural amino acids.

Directed evolution usually uses methods that target the entire protein and therefore favor distant mutations for statistical reasons. Only a few amino acid residues (<10%) form the substrate binding site, and most amino acid residues lie far away. Imagine a spherical enzyme with the active site at the center, in which the amino

*Correspondence: rjk@umn.edu

³Present address: University of British Columbia, Department of Biochemistry and Molecular Biology, Vancouver, British Columbia V6T 1Z3, Canada.

⁴Present address: Gyros AB, Uppsala Science Park, SE-75183 Uppsala, Sweden.

⁵Present address: University of Minnesota, Department of Biochemistry, Molecular Biology, and Biophysics and the Biotechnology Institute, 1479 Gortner Avenue, Saint Paul, Minnesota 55108.

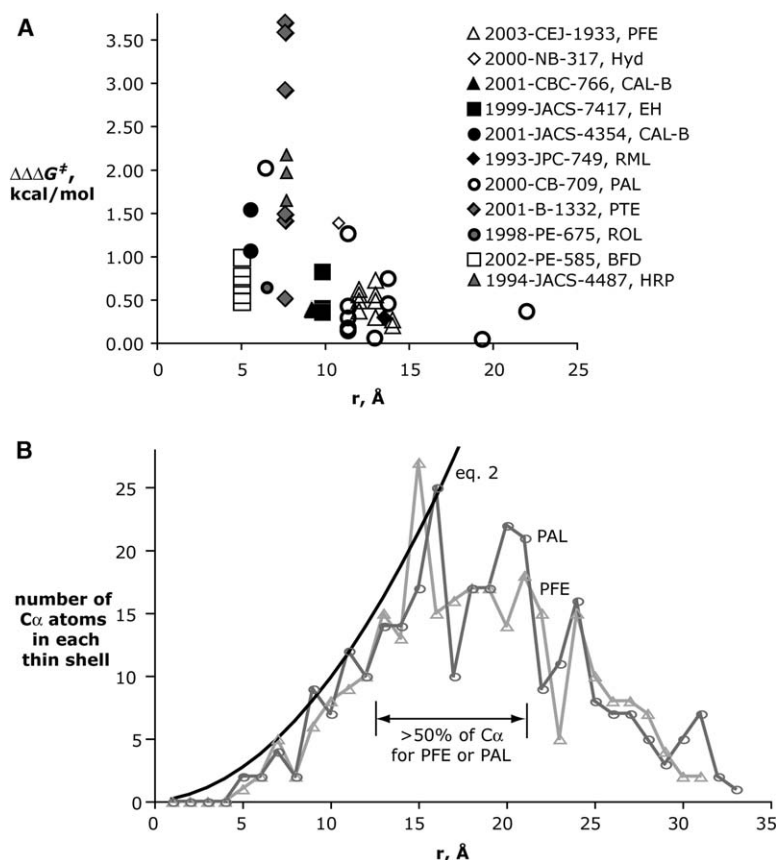


Figure 1. Single Mutations Closer to the Active Site Increase Enantioselectivity More Strongly than Single Distant Mutations, but Closer Amino Acids Are Rarer than Distant Ones

(A) Location of single mutations that increase enzyme enantioselectivity as identified by rational design (solid symbols) or directed evolution (outline symbols). The distance is from the C_α of the mutated amino acid to the stereocenter of the substrate bound to the enzyme or to a key active site residue. The closest contact may be shorter, depending on side chain orientations. The observed enantioselectivity changes are given as activation energy differences ($\Delta\Delta\Delta G^\ddagger$) to simplify comparison. Although the molecular details differ for each case, closer mutations increase enantioselectivity more strongly than distant mutations. The literature data for this figure are included as [Supplemental Data](#) (available with this article online).

(B) The number of amino acids in each 1 Å thick shell increases with the radius of the shell. The line shows the predicted values for a spherical enzyme with an active site in the center; see [Equation 2](#) in the text. The points correspond to the observed numbers in the X-ray crystal structures of lipase from *Pseudomonas aeruginosa* (PAL, circles) and esterase from *Pseudomonas fluorescens* (PFE, triangles). The distances are between C_α of the amino acid residues and the stereocenter of a modeled bound substrate (a 2-methyl carboxylic acid ester). The observed numbers fit the predicted line well up to ~ 16 Å, but are lower than predicted beyond

~ 16 Å because one reaches the edge of the protein. The number of amino acids is for each thin shell and is not cumulative. For this reason, it decreases as the shells extend beyond the protein. More than half of the amino acid residues in these enzymes are 13–22 Å from the active site, and $<10\%$ lie within 10 Å of the active site.

acid residues form concentric shells around the active site. As one moves outward, each shell contains more amino acids. The volume of each thin shell is the difference between the volume of a sphere with radius $r + d$ and the volume of a sphere with radius r (see [Equation 1](#)). The average number of amino acids within this shell is the volume divided by the average volume occupied by an amino acid residue, which is $141.3 \text{ Å}^3/\text{aa}$ (see [Equation 2](#)) [23].

$$V_{\text{thin shell}} = 4\pi \left(r_{\text{shell}}^2 d + r_{\text{shell}} d^2 + \frac{d^3}{3} \right) \quad (1)$$

$$N_{\text{aa in thin shell}} = \frac{4\pi \left(r_{\text{shell}}^2 d + r_{\text{shell}} d^2 + \frac{d^3}{3} \right)}{141.3 \text{ Å}^3 / \text{aa}} \quad (2)$$

This prediction agrees with values for 1 Å thick shells calculated from the X-ray structures of two typical enzymes of ~ 30 kDa (*Pseudomonas aeruginosa* lipase [24] and *Pseudomonas fluorescens* esterase [25]) up to ~ 16 Å ([Figure 1B](#)). The distance is between a key atom in the active site and the C_α of an amino acid residue. The side chain may be closer or farther depending on the direction in which it points. Beyond ~ 16 Å the observed numbers of amino acids are lower than predicted because one reaches the edge of the enzyme.

For these two examples, more than half of the amino acid residues lie 13–22 Å from the active site, and $<10\%$ lie within 10 Å of the active site. For larger proteins, the edges lie farther out, so most amino acids will lie even farther from the active site.

Practical considerations introduce bias into random mutagenesis methods such as error-prone PCR, DNA shuffling, and related methods. For example, transitions (substitutions between purines [A and G] or pyrimidines [T and C]) are more likely than traversions (substitutions between a purine and a pyrimidine) with error-prone PCR [26]. Similarly, crossovers at regions of high sequence similarity are more likely to occur when DNA shuffling is used [27]. This bias of DNA shuffling is desirable because it favors mutations that are most likely to yield a properly folded protein. However, beyond these biases, random mutagenesis methods that target the entire enzyme are biased toward distant mutations. The number of amino acid residues increases as one moves away from the active site, and the number of mutable positions increases as well. In a typical enzyme (~ 30 kDa), more than half of the amino acid residues lie 13–22 Å from the active site, so random mutagenesis that targets the entire enzyme favors mutations at this distance. For larger enzymes, the favored distance is even farther from the active site.

In this paper, we show that single random mutations

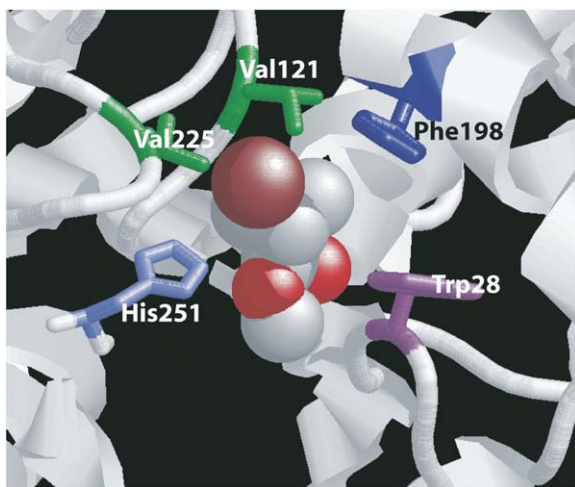


Figure 2. A Homology Model of PFE Containing the First Tetrahedral Intermediate in Hydrolysis of (*R*)-MBMP

Four residues, Trp28, Val121, Phe198, and Val225 (stick representation), lie close to the chiral acyl moiety of Ser94-MBMP (space-filling representation). The bromine (burgundy) of MBMP orients toward Val121. His251 is the catalytic histidine.

within the substrate binding site of *Pseudomonas fluorescens* esterase increase enantioselectivity for hydrolysis of methyl 3-bromo-2-methylpropionate (MBMP) more effectively than the method used in our previous work, which used single random mutations in the entire protein [15]. The fraction of mutants with increased enantioselectivity is much higher (13% versus <1%), and the changes are much larger (up to 5-fold versus 1.5-fold). Researchers have previously changed substrate specificity by using random mutations within the substrate binding site [28–31]. Our target substrate, MBMP, was chosen for three reasons. First, wild-type PFE showed moderate enantioselectivity toward this substrate ($E = 12[S]$). Second, MBMP is a useful bifunctional chiral building block [32–36]. Third, this resolution is a challenging one, and no good methods exist to resolve MBMP, as outlined in our previous paper [15]. For example, enzymatic kinetic resolution with a lipase from *Rhizopus delemar* has proceeded with only moderate enantioselectivity [32]. The current high price of enantiopure MBMP (US \$90/5 g [Aldrich], which corresponds to \$3300/mole) partly reflects this lack of a good route to this important compound.

Results

Selection of Sites for Saturation Mutagenesis

A homology model of PFE containing the first tetrahedral intermediate for hydrolysis of (*R*)-MBMP (slow-reacting enantiomer) revealed which amino acid residues are close to the substrate's stereocenter. The X-ray crystal structure of PFE, solved recently [25], is very similar to this homology model. We chose four positions for saturation mutagenesis: Trp28, Val121, Phe198, and Val225 (Figure 2). The PFE amino acids in an earlier publication [15] were numbered one higher

than here because the numbering included the initial methionine. The X-ray structure shows that the mature protein lacks this initial methionine. The side chains of Trp28 and Val225 lie on either side of the acyl binding region, while the side chains of Val121 and Phe198 lie above and behind the acyl binding region. All four of these amino acids are within van der Waals distance of the substrate (substrate stereocenter to amino acid C α distance is 5–7 Å), but two are also directly involved in the catalytic machinery. The backbone N-H of Trp28 stabilizes the tetrahedral intermediate by making a hydrogen bond to the oxyanion oxygen and the backbone N-H of Val225 stabilizes the side chain orientation of the catalytic Asp222 by making a hydrogen bond to O δ .

Mutagenesis and Identification of Catalytically Active Mutants

We introduced all 19 possible amino acids at the selected sites one at a time by saturation mutagenesis. This procedure involved copying DNA encoding for PFE by using polymerase chain extension of both plasmid strands with primers containing the degenerate codons at the selected site. The NNK codons gave 32 possible codons and coded for each of the 20 amino acids at least once. N represents any of the four nucleotides (A, T, G, or C); K represents either G or T. Transformation of this mixture of plasmids into *E. coli* gave a mixture of mutants (each transformation yielded >500 colonies). To ensure that we tested all 19 possible amino acid substitutions for Trp28 and Val121, we tested 192 colonies, which ensures that we tested >99.8% of the 32 possible codons (assuming equal incorporation) [37]. For the Phe198 library, we tested only 96 colonies, but this still ensures that we tested 95% of the possible codons. For the Val225 library, we screened many more colonies (480), since we did not find more enantioselective mutants at this position (see below) and wanted to be sure that we did not miss one.

To identify the catalytically active mutants, we screened for hydrolysis of *p*-nitrophenyl acetate. Approximately half of the mutants retained at least 1% of the catalytic activity of the wild-type (Figure 3A). Mutants with >10% of the wild-type activity were classified as active, those with 1%–10% of the wild-type activity were classified as less active, and those with <1% of the wild-type activity were classified as inactive. This initial assay used only crude enzyme solution, so that an active, but poorly expressed mutant would also be classified as inactive if the overall activity was <1%. While the Trp28 and Val225 libraries showed 37% and 35% active or less active colonies, respectively, the Phe198 and Val121 libraries contained 58% and 55% respectively. Consistent with our expectations, mutation of amino acid residues involved in catalytic machinery (Trp28 and Val225) gave a smaller proportion of active colonies than mutation of amino acid residues that only lie close to the active site. The total number of different mutants was 76 (19 amino acid substitutions at 4 sites). Since only approximately half of the colonies were active, we estimate that we created approximately 38 active mutants. To characterize these mutants, we screened approximately 1000 colonies to ensure that we tested each mutant.

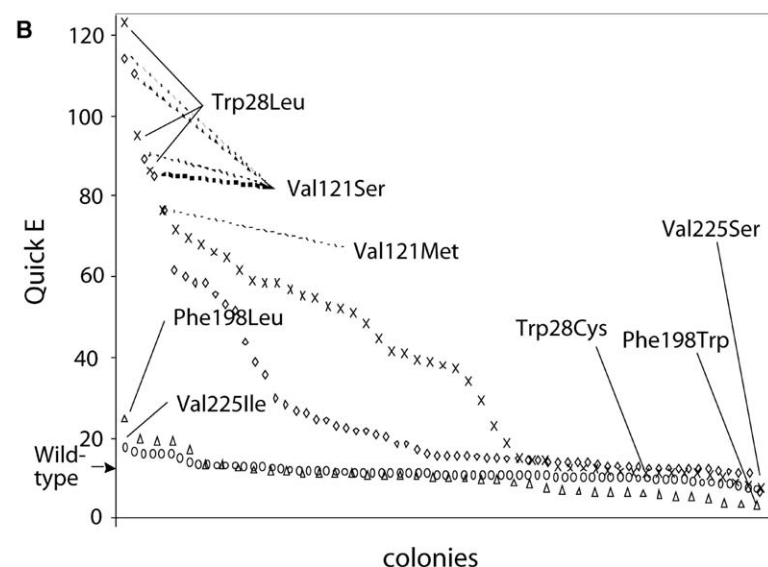
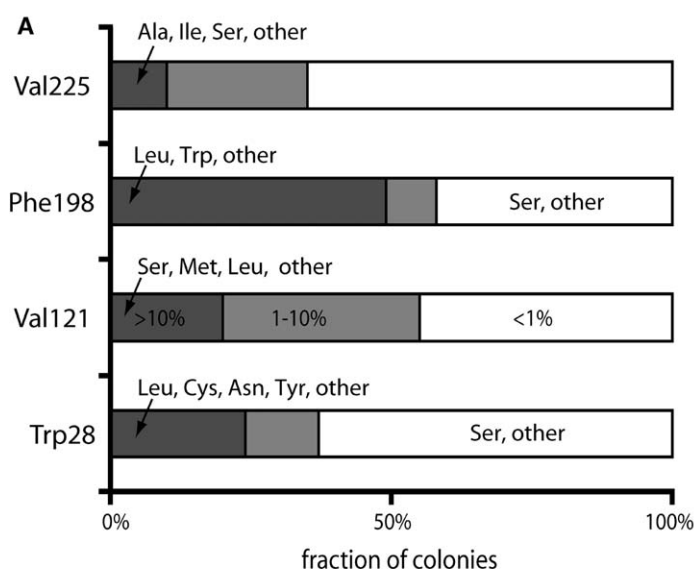


Figure 3. Activity and Enantioselectivity of PFE Mutant Colonies

(A) The fraction of colonies that catalyzed hydrolysis of *p*-nitrophenyl acetate after random mutagenesis at each of the four sites. Dark gray bars mark active colonies (>10% of the wild-type activity [WT activity = 1.6×10^{-3} $\mu\text{mol}/\text{min}/\mu\text{L}$]); light gray bars mark less active colonies (1%–10% of the wild-type activity); white bars mark inactive colonies (<1% of the wild-type activity). Val225, with only 15% active clones, was the least tolerant to mutations, while Phe198 was most tolerant (42% active).

(B) The enantioselectivity for colonies mutated at each site—28 ("X"), 121 (diamonds), 198 (triangles), and 225 (circles)—where the Quick E values describe the preferential hydrolysis of the *S*-enantiomer. Mutations at sites 198 and 225 show only small changes in enantioselectivity, while mutations at sites 28 and 121 showed dramatic increases in enantioselectivity. The range of Quick E values for some highly enantioselective mutants is large (e.g., Trp28Leu values range from 81 to 123) due to errors in measuring the very slow rate of hydrolysis of the slow-reacting enantiomer. The goal of this Quick E screening was only to identify which mutants were highly enantioselective, so we did not attempt to increase the accuracy of Quick E with highly enantioselective enzymes.

Enantioselectivity of Active Mutants

Colorimetric screening with Quick E [38–40] and DNA sequencing identified five mutants with increased enantioselectivity (Figure 3B). Both the Trp28 and Val121 libraries contained mutants with dramatically increased enantioselectivity, but the Phe198 and Val225 libraries contained mutants with only small changes in enantioselectivity. To confirm the enantioselectivity of mutants, we also measured the enantioselectivity by the endpoint method [41] (endpoint *E*) in small scale-up reactions with gas chromatography to measure the enantiomeric purity (Table 1). For the less enantioselective mutants, the Quick E values agreed with the endpoint *E*, but for the highly enantioselective mutants (*E* > 50), Quick E only identified that they were highly enantioselective and often overestimated the true enantioselectivity. These errors are due to difficulties measuring the very slow hydrolysis of the slow-reacting enantiomer.

The goal of this Quick E screening was only to identify which mutants were highly enantioselective, so we did not change reference compounds or make other adjustments that could increase the accuracy of Quick E with highly enantioselective enzymes.

Both the Val121 and Trp28 libraries showed numerous colonies that expressed PFE variants with high enantioselectivity (Quick *E* > 50); among these, we identified five unique mutants with significantly increased enantioselectivity. The most enantioselective mutants were Val121Ser (Quick *E* = 104), which gave an endpoint *E* of 61, and Trp28Leu (Quick *E* = 100), which gave an endpoint *E* of 58. This enantioselectivity is approximately 5-fold higher than the wild-type enantioselectivity of 12. Three other mutants with increased enantioselectivity were Val121Met (Quick *E* = 76, endpoint *E* = 36), Trp28Phe (Quick *E* = 39, endpoint *E* = 32), and Trp28Tyr (Quick *E* = 23, endpoint *E* = 29). Additional

Table 1. Enantioselectivity and Relative Activity toward MBMP of Wild-Type PFE and Variants Discovered by Saturation Mutagenesis within the Substrate Binding Site

Enzyme	Relative Rate ^a	Quick E^b	Endpoint E^b	$\Delta\Delta G^\ddagger$ (kcal/mol)	$\Delta\Delta\Delta G^\ddagger$ (kcal/mol)
Wild-type	1.0	11 \pm 0.9 ^c	12 \pm 2	1.5	0
Trp28Leu	1.6	100 \pm 20	58 \pm 7 ^d	2.4	0.93
Trp28Phe	0.84	39	32 \pm 1	2.1	0.58
Trp28Tyr	0.23	23	29 \pm 1	2.0	0.52
Trp28Cys	ND	11	ND ^e	ND	ND
Val121Ser	2.1	104 \pm 13	61 \pm 1	2.4	0.96
Val121Met	0.75	76	36 \pm 1	2.1	0.65
Phe198Leu	ND	25	10 \pm 1	1.4	-0.11
Phe198Trp	ND	3.0	2.2 \pm 0.5	0.48	-1.0
Val225Ala	ND	7.6	ND	ND	ND
Val225Ile	ND	16	ND	ND	ND
Val225Ser	ND	7.3	ND	ND	ND

^aHydrolysis toward the fast-reacting enantiomer using purified enzymes, which allowed the amount of protein to be normalized for each solution. Conditions: 7% acetonitrile; (S)-MBMP, 1.0 mM; BES-Na buffer (pH 7.2), 4.65 mM; Triton X-100, 0.292 mM; enzyme 0.031 mg/ml; *p*-nitrophenol, 0.42 mM; total volume, 100 μ l; 25°C.

^bIn all cases, PFE favors (S)-MBMP. Enantioselectivities were measured by using unpurified enzyme because the solution did not contain any other enzymes that catalyzed hydrolysis of MBMP.

^cErrors are standard deviations for at least three measurements; entries without errors are single measurements.

^dValues are the average of several measurements of enantioselectivity (E). Typical data are: 40% conversion, 62.9% enantiomeric excess for the remaining starting material, 92.6% enantiomeric excess for the product acid. These values correspond to an enantioselectivity of 50 when the equations in Chen et al. [41] are used.

^eND, not determined.

sequencing identified Trp28Cys as a mutant with enantioselectivity similar to wild-type (Quick E = 11 versus 12 for wild-type). The Phe198 and Val225 libraries contained only mutants with enantioselectivity similar to or lower than the wild-type: Val225Ile (Quick E = 16), Phe198Leu (Quick E = 25, endpoint E = 10), Phe198Trp (Quick E = 3, endpoint E = 2.2), Val225Ala (Quick E = 7.6), and Val225Ser (Quick E = 7.3). This total of 5 unique mutants with increased enantioselectivity is 13% of the estimated 38 unique active mutants in the library. This success rate is much higher than the typical <1% success rate seen when random mutagenesis throughout the protein is used.

Kinetic Parameters of the Two Best Mutants

Kinetic parameters show that the enantioselectivity in wild-type PFE stems from a lower k_{cat} for the slow-reacting *R*-enantiomer of MBMP. The K_M values are similar for both enantiomers (50 mM for [S] versus 80 mM for [R]), while k_{cat} is significantly higher for the fast-reacting enantiomer (1900 min⁻¹ for [S] versus 340 min⁻¹ for [R]). Other researchers also found a higher k_{cat} for the fast-reacting enantiomer for other serine hydrolases with chiral substrates [42, 43].

The two best mutations (Trp28Leu and Val121Ser) increased enantioselectivity by slightly increasing the reaction rate of the fast-reacting enantiomer, but mainly by further slowing the reaction rate of the slow-reacting enantiomer (Table 2). The k_{cat} values for the fast-reacting enantiomer (3500 min⁻¹ for Trp28Leu, 3300 min⁻¹ for Val121Ser) were about 2-fold higher than for wild-type (1900 min⁻¹), and the K_M values were all similar (70 mM for Trp28Leu, 40 for Val121Ser, 50 for wild-type). Thus, the specificity constants (k_{cat}/K_M) for the fast-reacting enantiomer increased slightly in the mutants: 51,000 min⁻¹M⁻¹ for Trp28Leu; 73,000 for Val121Ser compared to 36,000 for wild-type. For the slow-reacting enanti-

omer, the K_M values were again similar (80 mM for Trp28Leu, 100 for Val121Ser, 80 for wild-type), but the k_{cat} values decreased 4- to 5-fold in the mutants (70 min⁻¹ for Trp28Leu, 88 for Val121Ser, 340 for wild-type). This k_{cat} change lowered the specificity constants for the mutants: 820 min⁻¹M⁻¹ for Trp28Leu; 890 for Val121Ser compared to 4200 for wild-type.

Trp28Leu and Val121Ser Increase Enantioselectivity Mainly through Electronic Effects

To identify whether steric or electronic effects are the main reason for the increased enantioselectivity, we tested several substrate analogs, Table 3. The chloromethyl substituent in compound 2 has a smaller size but similar electronic characteristics to the bromomethyl substituent in MBMP (compound 1). If the enantioselectivity increase in the mutants stems mainly from electronic interactions, then there should be a similar increase for compound 2. Indeed, this was the case (Table 3). For Trp28Leu, the enantioselectivity increase from wild-type was 0.93 kcal/mol (from E = 12 to E = 58) for MBMP and 0.85 kcal/mol (from E = 11 to E = 46) for compound 2. For Val121Ser, the enantioselectivity increase from wild-type was 0.99 kcal/mol (from E = 12 to E = 61) for MBMP and 0.69 kcal/mol (from E = 11 to E = 35) for compound 2. These results suggest that the enantioselectivity increases of these mutants toward MBMP stem mainly from electronic interactions between the bromomethyl substituent and PFE.

To test the contribution of steric effects, we used compound 3, in which the isosteric methyl group replaces the bromo group of MBMP. (The van der Waals volumes of CH₄ and HBr are 17.1 and 17.9 cm³/mol, respectively [44].) If the enantioselectivity increase in the mutants stems mainly from steric interactions, then there should be a similar increase for compound 3. In

Table 2. Kinetic Parameters for the PFE-Catalyzed Hydrolysis of (S)- and (R)-MBMP

Enzyme	Enantiomer	k_{cat}^a (min ⁻¹)	K_M^a (mM)	k_{cat}/K_M (min ⁻¹ M ⁻¹)	$(k_{\text{cat}}/K_M)_S/(k_{\text{cat}}/K_M)_R^b$	Endpoint E
Wild-type	(S)	1,900	50	36,000	8.6	12
	(R)	340	80	4,200		
Trp28Leu	(S)	3,500	70	51,000	62	58
	(R)	70	80	820		
Val121Ser	(S)	3,300	40	73,000	82	61
	(R)	88	100	890		

^aAll measurements were performed four times under the following conditions: in a reaction well, 7% acetonitrile; BES buffer (pH 7.2), 4.65 mM; Triton X-100, 0.29 mM; PFE, 0.031 mg/ml for (S)-MBMP, but higher for (R)-MBMP; *p*-nitrophenol, 0.42 mM; total volume, 100 μ l; 25°C. Substrate concentration: 2.0–17 mM. The substrate did not dissolve above 17 mM.

^bThe values of $(k_{\text{cat}}/K_M)_S/(k_{\text{cat}}/K_M)_R$ should and do match the endpoint E values within the estimated error limits. We estimate at least $\pm 25\%$ error on each kinetic parameter, and thus the errors $(k_{\text{cat}}/K_M)_S/(k_{\text{cat}}/K_M)_R$ are at least $\pm 60\%$.

contrast with this prediction, we found little change in enantioselectivity of the mutants toward compound 3 (Table 3). For Trp28Leu, the enantioselectivity increase from wild-type was 0.93 kcal/mol (from $E = 12$ to $E = 58$) for MBMP, but only 0.04 kcal/mol (from $E = 32$ to $E = 34$) for compound 3. For Val121Ser, the enantioselectivity increase from wild-type was 0.99 kcal/mol (from $E = 12$ to $E = 61$) for MBMP and only 0.26 kcal/mol (from $E = 32$ to $E = 50$) for compound 3. These results suggest that steric effects do not contribute in the Trp28Leu mutation, but may contribute a small amount in the Val121Ser mutation. It is not obvious how the Val121Ser mutation could increase steric effects since the side chain of serine is smaller than that of valine.

Compound 4, which contains substituents of similar size but differing electronic character, was not a substrate for wild-type PFE, or any of the mutants. This lack of reactivity is consistent with a sterically restricted acyl binding site in PFE, as suggested by previous substrate mapping [45].

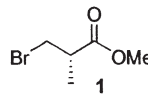
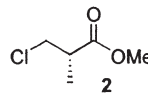
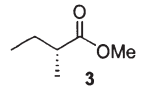
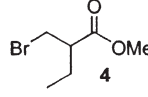
Proposed Molecular Basis for Enantioselectivity Increase

Of the three possible rotamers for the MBMP acyl moiety in the substrate binding site of PFE, we suggest

that only one of them is catalytically productive (Figure 4). During catalysis, the catalytic histidine forms a bifurcated hydrogen bond to the serine O γ and the OMe of the substrate. This requirement crowds the sector between these two groups; thus, we propose that only rotamers with a hydrogen in this sector (pointing down; Figure 4) are catalytically productive. The catalytically productive rotamer for the fast-reacting enantiomer orients the bromomethyl group toward Trp28, while, for the slow-reacting enantiomer, the bromomethyl group points toward Val121.

We propose that the Trp28Leu and Val121Ser mutations decrease k_{cat} for the slow-reacting enantiomer by selective destabilization of the transition state for this enantiomer by using mainly electronic interactions (Figure 4). The Trp28Leu mutation replaces Trp28 with a nonpolar amino acid. We propose that this change removes a repulsive electronic interaction between the electron-rich indole ring [46] of Trp28 and the electro-negative bromomethyl group and thus favors rotamers in which the bromomethyl group lies nearest position 28. For the fast-reacting enantiomer, this rotamer is reactive, while, for the slow-reacting enantiomer, it is unreactive. This favoring of unreactive rotamers destabilizes the transition state for the slow-reacting enantiomer. The Val121Ser mutation causes a similar destabi-

Table 3. Enantioselectivity Changes of PFE and Several Mutants toward MBMP (1) and Several Analogs

Substrate	Comment	E			$-\Delta\Delta\Delta G^\ddagger$ (kcal/mol)	
		Wild-Type	Trp28Leu	Val121Ser	Trp28Leu	Val121Ser
	standard	12 (S)	58 (S)	61 (S)	0.93	0.96
	similar electronic effects to 1	11 (S)	46 (S)	35 (S)	0.85	0.69
	similar steric effects to 1	32 (R)	34 (R)	50 (R)	0.04	0.26
		nr ^a	nr ^a	nr ^a	naa	na ^a

The configuration of the fast-reacting enantiomer is shown.

^aNeither wild-type nor any of the mutants catalyzed hydrolysis of compound 4. nr = no reaction; na = not applicable.

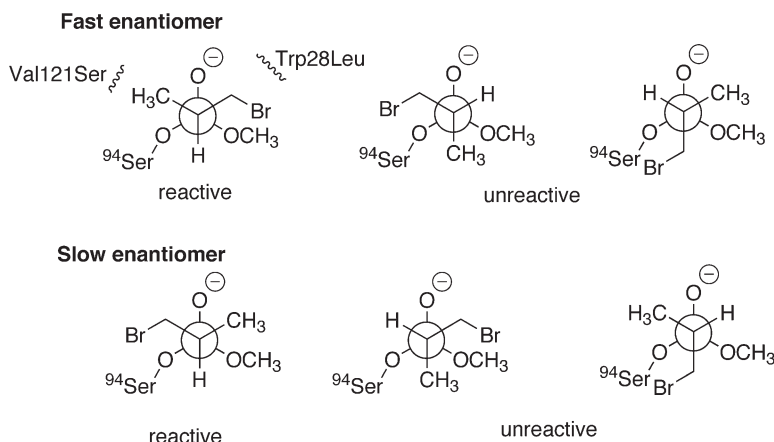


Figure 4. Proposed Orientation of MBMP in the Substrate Binding Site of PFE

During catalysis, the catalytic histidine (data not shown) forms a bifurcated hydrogen bond to the serine O_γ and the OMe of the substrate. This requirement crowds the sector between these two groups; thus, only rotamers with a hydrogen in this sector (pointing down) are reactive. Mutations that increase enantioselectivity favor unreactive orientations for the slow-reacting enantiomer, thereby destabilizing the transition state. The Val121Ser mutation introduces a repulsive interaction between Ser121 and the bromomethyl substituent, while the Trp28Leu mutation acts on the other side of the binding site to remove a repulsive interaction between Trp28 and the bromomethyl substituents. These changes favor the unreactive center rotamer for the slow-reacting enantiomer.

lization by adding a polar substituent on the other side of the binding site. We propose that this change adds a repulsive electronic interaction between the hydroxyl group of Ser121 and the bromomethyl group and thus also favors rotamers in which the bromomethyl group lies nearest position 28.

This rationale is also consistent with the increased enantioselectivity of other mutants at positions 28 and 121 and the decreased enantioselectivity of Phe198Trp (Table 1). Replacing Trp28 with aromatic amino acids (Phe, Tyr) gives a smaller enantioselectivity increase than the nonpolar Leu. Likewise, replacing Val121 with the slightly polar Met gives a smaller enantioselectivity increase than the more polar Ser. Position 198 lies near 28, so adding a Trp at position 198 is the reverse of the enantioselectivity-increasing mutations at position 28, which remove the Trp. Thus, the Phe198Trp mutant shows a lower enantioselectivity of 3. Rotticci et al. [47, 48] previously proposed a similar repulsive electronic interaction in *Candida antarctica* lipase B between the hydroxyl groups of Ser47 and Thr42 and the bromo substituent of 1-bromo-2-butanol.

Discussion

Saturation mutagenesis at four positions in the substrate binding site of PFE (Trp28, Val121, Phe198, and Val225) revealed five mutants (13% of active mutants) with higher enantioselectivity than wild-type enzyme. The enantioselectivity improved up to 5-fold. The best mutations, Val121Ser and Trp28Leu, increased enantioselectivity mainly by decreasing k_{cat} for the slow-reacting enantiomer by using electronic interactions.

Distant mutations can alter an enzyme's substrate selectivity and catalytic activity. The examples in Figure 1A show that single distant mutations can increase enantioselectivity. Hedstrom and coworkers demonstrated that, in addition to mutations in the substrate binding site, distant mutation of surface loops was essential to change the substrate specificity of trypsin (favors cleavage after Arg or Lys residues) to that of chymotrypsin (favors cleavage after Phe, Tyr, or Trp residues) [49–51]. Mutation of the substrate binding site alone deforms it [52] and yields a poor nonspecific protease. This simple mutation does alter the substrate

specificity as intended for ester hydrolysis, presumably because of the higher intrinsic reactivity of esters as compared to peptides. Similarly, adding remote substituents to the substrate can increase selectivity. For example, human leukocyte elastase favors Cbz-Val-pNP only 7-fold over Cbz-Phe-pNP, but it favors Boc-Ala-Ala-Val-SBzl more than 10^5 -fold over Boc-Ala-Ala-Phe-Sbzl [53]. Arkin and Wells showed that two distant (second-sphere) mutations increased the catalytic activity (k_{cat}/K_M) of an esterolytic catalytic antibody 10-fold [54].

Are single distant mutations the best way to increase enantioselectivity? One advantage of single distant mutations may be smaller disruptions of the enzyme's active site. Distant mutations can propagate structural changes to the active site, where they cause subtle structural changes. Subtle structural changes can significantly change the reaction rate. For example, small (~ 1 Å) shifts in the active site dramatically changed the catalytic power of isocitrate dehydrogenase [55, 56]. Closer mutations make larger changes that may disrupt catalytic activity or enantioselectivity. Indeed, when we mutated amino acids in the substrate binding site, approximately half of our mutants were inactive.

In spite of the possible advantages of distant mutations, we suggest that directed evolution with random mutagenesis of the entire enzyme usually identifies distant mutations, not because they are better, but because they are more likely. A complete screening identifies the best mutants, but most directed evolution experiments do not screen every mutant generated because it is easier to make mutants than it is to screen them. In these cases, the mutants identified depend both on their likelihood of being formed and their ability to increase enantioselectivity. One directed evolution experiment in which the researchers did screen all possible single mutants indeed identified a mutation close to the active site, not a distant mutation. Using degenerate DNA primers, Desantis and coworkers introduced all 19 alternate amino acids at each targeted position of a nitrilase. Homology models showed that mutants with the highest increases in enantioselectivity had mutations close to the active site [57].

To increase enantioselectivity, several lines of evidence suggest that single closer mutations are more effective than single distant mutations. Previously, we

used random mutagenesis on the entire PFE to identify more enantioselective mutants. We found single distant mutations that moderately increased enantioselectivity. In the current work, mutations targeted to the substrate binding site increase both the fraction of mutations with increased enantioselectivity and the size of the increase. Koga and coworkers [17] reported a similar strategy to invert the enantioselectivity of *Burkholderia cepacia* KWI-56 lipase. Simultaneous mutation of four amino acids yielded a mutant with high enantioselectivity for the opposite enantiomer. Rational design to increase enzyme enantioselectivity focuses on close mutations and yields much larger changes than designs that use distant mutations (see Figure 1). Finally, chemical catalysts and enzymes use the same physical principles to distinguish enantiomers. Computational and experimental studies with organometallic catalysts show that stereodirecting groups close to the reaction center give higher enantioselectivity than distant ones [58].

Our approach does not require a detailed structure of the enzyme to work effectively. In our case, a homology model was generated to learn the basic structure of the substrate binding site of PFE. For instances in which a homology model is not available, a more simplified approach would be to select positions for mutagenesis from the amino acid sequence of the enzyme based on proximity to the catalytic positions (i.e., Ser, His, Asp for lipases/esterases). Overall, this strategy looks promising as a general method to increase the enantioselectivity of enzymes. For improving other properties, like organic solvent stability, that are not yet understood on a molecular basis, random mutagenesis throughout the entire protein would be the more promising approach. These properties may require mutations distributed throughout the protein structure, and there is no evidence suggesting that active site mutations would be more effective in these cases.

Significance

Random mutagenesis of an entire enzyme creates more mutations far from the active site than close to the active site because there are more amino acids far from the active site than close to the active site. In a typical enzyme, <10% of the amino acid residues are within the substrate binding site, while more than half lie 13–22 Å away. If one generates and tests every single amino acid mutant, one finds the best one regardless of its location. However, incomplete screening of libraries targeting the entire enzyme favors distant mutations. This bias toward distant mutations has not been fully recognized. This work showed that mutations close to the active site caused larger and more frequent increases in enantioselectivity than distant mutations previously identified by random mutagenesis of the entire enzyme. This work suggests that random mutagenesis focused on the substrate binding site is a more efficient strategy than targeting the whole enzyme to improve catalytic properties such as enantioselectivity.

Experimental Procedures

General

Chemicals, buffers, and lysozyme were purchased from Sigma-Aldrich (Oakville, ON). LB media was obtained from Difco Laborato-

ries (Detroit, MI). RNase A was from USB Corporation (Cleveland, OH) and DNase I was purchased from Invitrogen Canada Inc. (Burlington, ON). The Sheldon Biotechnology Center (McGill University, Montréal, QC) made the primers and sequenced the mutants by using dideoxy termination sequencing.

Homology Model Containing MBMP Tetrahedral Intermediate

This model was created as previously described [15], by using the SWISS-MODEL automated homology-modeling server [59]. This model agrees with the X-ray crystal structure of this esterase, which was solved recently [25]. Figure 2 was prepared with Ras-Mol [60].

Saturation Mutagenesis

Using the vector pJOE2792 [61, 62] as a template, the QuikChange Site-Directed Mutagenesis Kit (Stratagene, La Jolla, CA) was used according to the manufacturer's instructions to construct the four libraries with complementary primers W28 (5'-GGTGTGTTTCAGCCACGGTNNKCTACTGGATGCCGACATGTGG-3'), cW28 (5'-CCACA TGTCGGCATCCAGTAGMNNACCGTGGCTGAACAACACC-3'), V121 (5'-CCTGGTGCTGCTGGCGCCNNKACCCGCTGTTCGGCCAGAGC-3'), cV121 (5'-GCTTCTGGCCGAACAGCGGGTMMNNGCGCACCAGCAGCACCAGG-3'), F198 (5'-GGTGGATTGCGTCACCGCGNNKGCCGAAACCGACTTCCGC-3'), cF198 (5'-GCGGAAGTCGGTTTCGGCMNNCGCGGTGACGCAATCCACC-3'), V225 (5'-GGCGATGGCGACCAGATCNNKCCGTTTCGAGACCACCGGC-3'), and cV225 (5'-GCCGGTGGTCTCGAACGGMNNGATCTGGTCGCCATCGCC-3'). The plasmid library of saturation mutants was transformed into *E. coli* DH5 α . If needed, the transformation was repeated to get >500 colonies, and colonies were transferred from LB agar plates containing ampicillin (100 μ g/ml) to 96-well microplates for overnight growth at 37°C in LB medium (100 μ l; ampicillin, 100 μ g/ml). Overnight culture was used fresh for further experiments, and remaining culture was stored in 50% (v/v) glycerol at -20°C.

Enzyme Production in 96-Well Format

To hasten the process of protein expression and isolation and thus facilitate the screening of large numbers of enzymes, bacteria were cultured in 96-well assay blocks (Costar, Cambridge, MA) as previously described [15]; each well had a total available volume of 2 ml. Fresh overnight culture from microplates (10 μ l) was added to each well containing LB medium (1 ml; ampicillin, 100 μ g/ml), and the assay block was incubated at 37°C and 325 rpm for approximately 3 hr, after which time the OD₆₀₀ was estimated to be 0.5. Protein expression was then induced by the addition of sterile rhamnose solution to each well (50 μ l; 4% w/v), followed by incubation as described above for 6 hr. The assay blocks were centrifuged (10 min, 2700 \times g, 4°C), and the supernatant was removed. The cell pellet was resuspended in *N,N*-bis[2-hydroxyethyl]-2-aminoethanesulfonic acid (BES) buffer (400 μ l; 5 mM [pH 7.2]; lysozyme, 0.4 mg/ml) and incubated at 37°C and 325 rpm for 45 min, followed by freezing at -20°C. After thawing at room temperature, the lysed cells were treated with nucleases (RNase A, 10 μ g/ml; DNase I, 1.7 μ g/ml) for 15 min at 37°C and 325 rpm, and then centrifuged (30 min, 2700 \times g, 4°C). The supernatant was used for further experiments. Quick E control experiments ensured that no detectable hydrolysis of MBMP occurred due to the nucleases, lysozyme, or cell-free extracts of nontransformed DH5 α .

Quick E Screening toward MBMP

Enzymatic hydrolyses of pure enantiomers of MBMP were monitored colorimetrically in the presence of a reference compound as previously described [40]. Rates of hydrolysis at 25°C of substrate (11 mM *R*-enantiomer or 1.1 mM *S*-enantiomer) and resorufin acetate (0.11 mM) or resorufin isobutyrate (0.03 mM) in buffer solution (100 μ l; BES, 5 mM [pH 7.2]; Triton X-100, 0.33 mM; acetonitrile, 8% v/v; *p*-nitrophenol, 0.42 mM; enzyme solution, 10% v/v) were determined from the change in absorbance at 404 and 574 nm as a function of time by using a microplate reader.

Purification of PFE

To determine enantioselectivity by the endpoint method, pure PFE enzyme was desirable so as to avoid competing hydrolysis from any other enzymes that may be present in the crude preparation.

The His₆ tag present on the C terminus of PFE allowed easy purification with Ni-NTA agarose resin according to the manufacturer's protocol (Qiagen Inc., Mississauga, ON). Overnight culture (1 ml) was added to LB medium (100 ml; ampicillin, 100 µg/ml) and grown at 37°C and 200 rpm to an OD₆₀₀ of 0.5. Protein expression was induced by the addition of sterile rhamnose (800 µl; 20% w/v) and incubation for 6 hr at 37°C and 200 rpm. The cells were harvested by centrifugation (10 min, 3800 × g, 4°C), and the supernatant was discarded. The cell pellet was resuspended in Buffer A (5 ml/g wet weight; NaH₂PO₄, 50 mM; NaCl, 300 mM; imidazole, 10 mM; adjusted to pH 8.0 with NaOH), and lysozyme was added to 1 mg/ml. Incubation at 37°C and 200 rpm for 30 min was followed by a freeze-thaw cycle at -20°C and room temperature.

The viscosity of the lysate was broken by repeatedly passing the solution through a sterile 20-gauge syringe needle, and the sample was centrifuged (10 min, 10,000 × g, 4°C). Ni-NTA agarose resin to a final concentration of 20% (v/v) was added to the supernatant, and the mixture was stirred at 4°C for 1 hr. The mixture was loaded onto a Poly-Prep column (BioRad Laboratories, Mississauga, ON), drained, and then washed two times with Buffer B (4 ml; NaH₂PO₄, 50 mM; NaCl, 300 mM; imidazole, 20 mM; adjusted to pH 8.0 with NaOH). The His₆-PFE enzyme was eluted from the column with 4 volumes of Buffer C (0.5 ml; NaH₂PO₄, 50 mM; NaCl, 300 mM; imidazole, 250 mM; adjusted to pH 8.0 with NaOH).

Elate (2 ml) from the Ni-NTA column containing purified PFE was exchanged from Buffer C to BES (5 mM [pH 7.2]) by using a Slide-a-Lyzer (Pierce, Rockford, IL) as per the manufacturer's instructions.

Confirmation of Enantioselectivity by Endpoint Method

Enantioselectivity of the hydrolysis of (±)-MBMP was calculated by using the method of Chen et al. [41] from the enantiomeric excesses of both starting ester and esterified acid product determined by GC on a chiral stationary phase as previously described [45].

Supplemental Data

Supplemental Data including two tables listing all of the literature, data, and references used to make Figure 1 are available at <http://www.chembiol.com/cgi/content/full/12/1/45/DC1/>.

Acknowledgments

We thank the Natural Sciences and Engineering Research Council of Canada for financial support and a fellowship to K.L.M. and the Swedish Foundation for International Cooperation in Research and Development for financial support. We thank Prof. Dr. Uwe T. Bornscheuer (Ernst-Moritz-Arndt-University, Greifswald, Germany) for the expression plasmid for PFE and Linda Fransson (Royal Institute of Technology, Stockholm, Sweden) for assistance in constructing the homology model.

Received: August 7, 2004

Revised: September 24, 2004

Accepted: October 13, 2004

Published: January 21, 2005

References

- Reetz, M.T. (2004). Controlling the enantioselectivity of enzymes by directed evolution: practical and theoretical ramifications. *Proc. Natl. Acad. Sci. USA* 101, 5716–5722.
- Robertson, D.E., and Steer, B.A. (2004). Recent progress in biocatalyst discovery and optimization. *Curr. Opin. Chem. Biol.* 8, 141–149.
- Dalby, P.A. (2003). Optimizing enzyme function by directed evolution. *Curr. Opin. Struct. Biol.* 13, 500–505.
- Cherry, J.R., and Fidantsef, A.L. (2003). Directed evolution of industrial enzymes: an update. *Curr. Opin. Biotechnol.* 14, 438–443.
- Chen, R. (2001). Enzyme engineering: rational redesign versus directed evolution. *Trends Biotechnol.* 19, 13–14.
- Bornscheuer, U.T., and Pohl, M. (2001). Improved biocatalysts

- by directed evolution and rational protein design. *Curr. Opin. Chem. Biol.* 5, 137–143.
- Jaeger, K.-E., Eggert, T., Eipper, A., and Reetz, M.T. (2001). Directed evolution of an enantioselective lipase. *Appl. Microbiol. Biotechnol.* 55, 519–530.
- Petrounia, I.P., and Arnold, F.H. (2000). Designed evolution of enzymatic properties. *Curr. Opin. Biotechnol.* 11, 325–330.
- Arnold, F.H. (1996). Directed evolution - creating biocatalysts for the future. *Chem. Eng. Sci.* 51, 5091–5102.
- Arnold, F.H. (1998). Design by directed evolution. *Acc. Chem. Res.* 31, 125–131.
- Reetz, M.T., Zonta, A., Schimossek, K., Liebeton, K., and Jaeger, K.-E. (1997). Creation of enantioselective biocatalysts for organic chemistry by in vitro evolution. *Angew. Chem. Int. Ed. Engl.* 36, 2830–2832.
- Liebeton, K., Zonta, A., Schimossek, K., Nardini, M., Lang, D., Dijkstra, B.W., Reetz, M.T., and Jaeger, K.-E. (2000). Directed evolution of an enantioselective lipase. *Chem. Biol.* 7, 709–718.
- May, O., Nguyen, P.T., and Arnold, F.H. (2000). Inverting enantioselectivity by directed evolution of hydantoinase for improved production of L-methionine. *Nat. Biotechnol.* 18, 317–320.
- Bornscheuer, U.T., Altenbuchner, J., and Meyer, H.H. (1999). Directed evolution of an esterase: screening of enzyme libraries based on pH-indicators and a growth assay. *Bioorg. Med. Chem.* 7, 2169–2173.
- Horsman, G.P., Liu, A.M.F., Henke, E., Bornscheuer, U.T., and Kazlauskas, R.J. (2003). Mutations in distant residues moderately increase the enantioselectivity of *Pseudomonas fluorescens* esterase toward methyl 3-bromo-2-methylpropanoate and ethyl 3-phenylbutyrate. *Chem. Eur. J.* 9, 1933–1939.
- Reetz, M.T., Torre, C., Eipper, A., Lohmer, R., Hermes, M., Brunner, B., Maichele, A., Bocola, M., Arand, M., Cronin, A., Genzel, Y., Archelas, A., and Furstoss, R. (2004). Enhancing the enantioselectivity of an epoxide hydrolase by directed evolution. *Org. Lett.* 6, 177–180.
- Koga, Y., Kato, K., Nakano, H., and Yamane, T. (2003). Inverting enantioselectivity of *Burkholderia cepacia* KWL-56 lipase by combinatorial mutation and high-throughput screening using single-molecule PCR and *in vitro* expression. *J. Mol. Biol.* 337, 585–592.
- Scheib, H., Pleiss, J., Stadler, P., Kovac, A., Potthoff, A.P., Haalck, L., Spener, F., Paltauf, F., and Schmid, R.D. (1998). Rational design of *Rhizopus oryzae* lipase with modified stereoselectivity toward triacylglycerols. *Protein Eng.* 11, 675–682.
- Rotticci, D., Rotticci-Mulder, J.C., Denman, S., Norin, T., and Hult, K. (2001). Improved enantioselectivity of a lipase by rational protein engineering. *ChemBioChem* 2, 766–770.
- Magnusson, A., Hult, K., and Holmquist, M. (2001). Creation of an enantioselective hydrolase by engineered substrate-assisted catalysis. *J. Am. Chem. Soc.* 123, 4354–4355.
- Rink, R., Spelberg, J.H.L., Pieters, R.J., Kingma, J., Nardini, M., Kellogg, R.M., Dijkstra, B.W., and Janssen, D.B. (1999). Mutation of tyrosine residues involved in the alkylation half reaction of epoxide hydrolase from *Agrobacterium radiobacter* AD1 results in improved enantioselectivity. *J. Am. Chem. Soc.* 121, 7417–7418.
- Chen-Goodspeed, M., Sogorb, M.A., Wu, F., and Raushel, F.M. (2001). Enhancement, relaxation, and reversal of the stereoselectivity for phosphotriesterase by rational evolution of active site residues. *Biochemistry* 40, 1332–1339.
- Zamyatin, A.A. (1972). Protein volume in solution. *Prog. Biophys. Mol. Biol.* 24, 107–123.
- Nardini, M., Lang, D.A., Liebeton, K., Jaeger, K.-E., and Dijkstra, B.W. (2000). Crystal structure of *Pseudomonas aeruginosa* lipase in the open conformation. The prototype for family I.1 of bacterial lipases. *J. Biol. Chem.* 275, 31219–31225.
- Cheeseman, J.D., Tocilj, A., Park, S., Schrag, J.D., and Kazlauskas, R.J. (2004). X-Ray crystal structure of an aryl esterase from *Pseudomonas fluorescens*. *Acta Crystallogr. D Biol. Crystallogr.* 60, 1237–1243.
- Fromant, M., Blanquet, S., and Plateau, P. (1995). Direct random mutagenesis of gene sized DNA fragments using polymerase chain reaction. *Anal. Biochem.* 224, 347–353.
- Ness, J.E., Kim, S., Gottman, A., Pak, R., Krebber, A., Borchert,

- T.V., Govindarajan, S., Mundorff, E.C., and Minshull, J. (2002). Synthetic shuffling expands functional protein diversity by allowing amino acids to recombine independently. *Nat. Biotechnol.* 20, 1251–1255.
28. Whittle, E., and Shanklin, J. (2001). Engineering $\Delta 9$ –16:0-acyl carrier protein (ACP) desaturase specificity based on combinatorial saturation mutagenesis and logical redesign of the castor $\Delta 9$ –18:0-ACP desaturase. *J. Biol. Chem.* 276, 21500–21505.
29. Li, Q.-S., Schwaneberg, U., Fischer, M., Schmitt, J., Pleiss, J., Lutz-Wahl, S., and Schmid, R.D. (2001). Rational evolution of a medium chain-specific cytochrome P-450 BM-3 variant. *Biochim. Biophys. Acta* 1545, 114–121.
30. Yang, J., Koga, Y., Nakano, H., and Yamane, T. (2002). Modifying the chain-length selectivity of the lipase from *Burkholderia cepacia* KWI-56 through in vitro combinatorial mutagenesis in the substrate-binding site. *Protein Eng.* 15, 147–152.
31. Graham, L.D., Haggett, K.D., Jennings, P.A., Le Brocque, D.S., and Whittaker, R.G. (1993). Random mutagenesis of the substrate-binding site of a serine protease can generate enzymes with increased activities and altered primary specificities. *Biochemistry* 32, 6250–6258.
32. Elferink, V.H.M., Kierkels, J.G.T., Kloosterman, M., and Roskam, J.H. May 1990. Enzyme process for the enantioselective preparation of d-(-)-3-halo-2-methylpropionic acid or derivatives thereof and the preparation of captopril therefrom. European patent 369553.
33. Sikorski, J.A., Getman, D.P., Decrescenzo, G.A., Devadas, B., Freskos, J.N., Lu, H.-T., and McDonald, J.J. May 1997. Preparation of N-[2-hydroxy-4-phenyl-3-(sulfonylalkanoylamino)butyl]arylsulfonamides and analogs as retroviral protease inhibitors. World patent 9718205.
34. Fadel, A., and Khesrani, A. (1998). A straightforward synthesis of both enantiomers of *allo*-norcoronamic acids and *allo*-coronamic acids by asymmetric Strecker reaction from alkylcyclopropanone acetals. *Tetrahedron. Asymmetry* 9, 305–320.
35. Tait, A., Colorni, E., and Di Bella, M. (1996). Stereospecific synthesis of 3-[(2*H*-1,2,4-benzothiadiazine-1,1-dioxide-3-yl)thio]-2-methylpropanoic acids. *Tetrahedron Asymmetry* 7, 2703–2706.
36. Czeskis, B.A., and Moissenkov, A.M. (1989). Synthesis of the S-enantiomer of paniculidone A: absolute R-configuration of the natural paniculidones A and B. *J. Chem. Soc., Perkin Trans. 1* 1, 1353–1354.
37. Warren, M.S., and Benkovic, S.J. (1997). Combinatorial manipulation of three key active site residues in glycinamide ribonucleotide transformylase. *Protein Eng.* 10, 63–68.
38. Janes, L.E., and Kazlauskas, R.J. (1997). Quick E. A fast spectrophotometric method to measure the enantioselectivity of hydrolases. *J. Org. Chem.* 62, 4560–4561.
39. Janes, L.E., Löwendahl, A.C., and Kazlauskas, R.J. (1998). Quantitative screening of hydrolase libraries using pH indicators: identifying active and enantioselective hydrolases. *Chemistry* 4, 2317–2324.
40. Janes, L.E., Cimpola, A., and Kazlauskas, R.J. (1999). Protease-mediated separation of cis and trans diastereomers of 2-(*R,S*)-benzyloxymethyl-4-(*S*)-carboxylic acid-1,3-dioxolane methyl ester: intermediates for the synthesis of dioxolane nucleosides. *J. Org. Chem.* 64, 9019–9029.
41. Chen, C.S., Fujimoto, Y., Girdaukas, G., and Sih, C.J. (1982). Quantitative analyses of biochemical kinetic resolutions of enantiomers. *J. Am. Chem. Soc.* 104, 7294–7299.
42. Nishizawa, K., Ohgami, Y., Matsuo, N., Kisida, H., and Hirohara, H. (1997). Studies of hydrolysis of chiral, achiral and racemic alcohol esters with *Pseudomonas cepacia* lipase: mechanism of stereospecificity of the enzyme. *J. Chem. Soc., Perkin Trans. 1* 2, 1293–1298.
43. Ema, T., Kobayashi, J., Maeno, S., Sakai, T., and Utaka, M. (1998). Origin of the enantioselectivity of lipases explained by a stereo-sensing mechanism operative at the transition state. *Bull. Chem. Soc. Jpn.* 71, 443–453.
44. Yaws, C.L. <http://www.knovel.com/knovel2/Toc.jsp?BookID=49> (2002).
45. Liu, A.M.F., Somers, N.A., Kazlauskas, R.J., Brush, T.S., Zocher, F., Enzelberger, M.M., Bornscheuer, U.T., Horsman, G.P., Metzger, A., Schmidt-Dannert, C., et al. (2001). Mapping the substrate selectivity of new hydrolases using colorimetric screening: lipases from *Bacillus thermocatenulatus* and *Ophiostoma piliferum*, esterases from *Pseudomonas fluorescens* and *Streptomyces diastatochromogenes*. *Tetrahedron Asymmetry* 12, 545–556.
46. Alagona, G., Ghio, C., and Monti, S. (1998). The effect of small substituents on the properties of indole. An ab initio 6–31G* study. *Theochem* 433, 203–216.
47. Rotticci, D., Rotticci-Mulder, J.C., Denman, S., Norin, T., and Hult, K. (2001). Improved enantioselectivity of a lipase by rational protein engineering. *ChemBioChem* 2, 766–770.
48. Rotticci, D., Orrenius, C., Hult, K., and Norin, T. (1997). Enantiomerically enriched bifunctional sec-alcohols prepared by *Candida antarctica* lipase B catalysis. Evidence of non-steric interactions. *Tetrahedron Asymmetry* 8, 359–362.
49. Hedstrom, L., Szilagyi, L., and Rutter, W.J. (1992). Converting trypsin to chymotrypsin: the role of surface loops. *Science* 255, 1249–1253.
50. Hedstrom, L. (1996). Trypsin: a case study in the structural determinants of enzyme specificity. *Biol. Chem.* 377, 465–470.
51. Hedstrom, L. (2002). Serine protease mechanism and specificity. *Chem. Rev.* 102, 4501–4523.
52. Szabó, E., Böcskei, Z., Náray-Szabó, G., and Gráf, L. (1999). The three-dimensional structure of Asp189Ser trypsin provides evidence for an inherent structural plasticity of the protease. *Eur. J. Biochem.* 263, 20–26.
53. Stein, R.L. (1985). Catalysis by human leukocyte elastase: III. Steady-state kinetics for the hydrolysis of p-nitrophenyl esters. *Arch. Biochem. Biophys.* 236, 677–680.
54. Arkin, M.R., and Wells, J.A. (1998). Probing the importance of second sphere residues in an esterolytic antibody by phage display. *J. Mol. Biol.* 284, 1083–1094.
55. Mesecar, A.D., Stoddard, B.L., and Koshland, D.E., Jr. (1997). Orbital steering in the catalytic power of enzymes: small structural changes with large catalytic consequences. *Science* 277, 202–206.
56. Koshland, D.E., Jr. (1998). Conformational changes: how small is big enough? *Nat. Med.* 4, 1112–1114.
57. DeSantis, G., Wong, K., Farwell, B., Chatman, K., Zhu, Z., Tomlinson, G., Huang, H., Tan, X., Bibbs, L., Chen, P., et al. (2003). Creation of a productive, highly enantioselective nitrilase through gene site saturation mutagenesis (GSSM). *J. Am. Chem. Soc.* 125, 11476–11477.
58. Lipkowitz, K.B., D'Hue, C.A., Sakamoto, T., and Stack, J.N. (2002). Stereocartography: a computational mapping technique that can locate regions of maximum stereoselection around chiral catalysts. *J. Am. Chem. Soc.* 124, 14255–14267.
59. Guex, N., Diemand, A., and Peitsch, M.C. (1999). Protein modelling for all. *Trends Biochem. Sci.* 24, 364–367.
60. Sayle, R.A., and Milner-White, E.J. (1995). RASMO: biomolecular graphics for all. *Trends Biochem. Sci.* 20, 374–376.
61. Krebsfänger, N., Zocher, F., Altenbuchner, J., and Bornscheuer, U.T. (1998). Characterization and enantioselectivity of a recombinant esterase from *Pseudomonas fluorescens*. *Enzym. Microb. Technol.* 22, 641–646.
62. Krebsfänger, N., Schierholz, K., and Bornscheuer, U.T. (1998). Enantioselectivity of a recombinant esterase from *Pseudomonas fluorescens* towards alcohols and carboxylic acids. *J. Biotechnol.* 60, 105–112.